

The role of the strain induced population imbalance in Valley polarization of graphene: Berry curvature perspective

Tohid Farajollahpour^{1,2} and Arash Phirouznia^{1,2,*}

¹Department of Physics, Azarbaijan Shahid Madani University, 53714-161, Tabriz, Iran

²Condensed Matter Computational Research Lab. Azarbaijan Shahid Madani University, 53714-161, Tabriz, Iran
*phirouznia@azaruniv.edu

ABSTRACT

Real magnetic and lattice deformation gauge fields have been investigated in honeycomb lattice of graphene. The coexistence of these two gauges will induce a gap difference between two valley points (K and K') of system. This gap difference allows us to study the possible topological valley Hall current and valley polarization in the graphene sheet. In the absence of magnetic field, the strain alone could not generate a valley polarization when the Fermi energy coincides exactly with the Dirac points. Since in this case there is not any imbalance between the population of the valley points. In other words each of these gauges alone could not induce any topological valley-polarized current in the system at zero Fermi energy. Meanwhile at non-zero Fermi energies population imbalance can be generated as a result of the external strain even at zero magnetic field. In the context of Berry curvature within the linear response regime the valley polarization (both magnetic free polarization, Π_0 , and field dependent response function, χ_α) in different values of gauge fields of lattice deformation has been obtained.

Valleytronics, the valley version of spintronics is based on quantum valley number which carries the information by valley degree of freedom.¹ The family of two dimensional materials with hexagonal lattice structures are potentially a good candidate to manipulate valley polarization.¹⁻⁷ Recently the first observation of valley Hall effect in graphene family with inversion symmetry breaking has been reported.^{8,9} Various proposals have been presented for generation of the valley Hall conductivity.¹⁰ Massive Dirac electrons in graphene has been suggested for valleytronics applications.^{11,12} In the literatures, most of the proposals for valley-filtering realization are combinations of strain induced gauge fields and electromagnetic fields.¹³⁻¹⁷ A valley filter has been proposed regarding the fact that the effective magnetic field (that results from combination of the strain and external magnetic field) is large in one of the Dirac cones and can be zero in the other.¹⁷ In the presence of Rashba spin orbit coupling and magnetic barrier in strained graphene, it is possible to produce valley and spin polarized currents.¹⁸ Jiang and *et al* proposed a scheme for generation of valley current in strained graphene in which the strain could be described by cyclic adiabatic deformations and there is a chemical potential in suspended region.¹⁹ Wang and *et al* have used the method of adiabatic quantum pumping in a three barrier structure with strained graphene and a ferromagnetic layer to generate pure valley current.²⁰

The heart of the field of straintronic in two dimensional materials is to manipulate the valley polarization by applying various deformations. The possibility of strain induced pseudomagnetic field in graphene family up to 300 T is a remarkable result and getting attention to strain engineering in graphene-like systems.²¹⁻²³ Further challenges for generating pseudomagnetic fields in graphene and other two dimensional materials not restricted to locally strained graphene nanobubbles. There is recently another proposal by Zhu and coworkers in which a pseudomagnetic field around 200 T has been obtained by an uniaxial stretched graphene.²³ Arias and coworkers considered the possibility of gauge field generation from an elastic deformation in graphene by a quantum field theory approach. They found a relation between the pseudomagnetic field and Riemann curvature.²⁴ Vaezi and coworkers by means of time dependent strain and consequently a time dependent gauge field showed that the charge current could be generated due to the time dependent elastic deformations in graphene.²⁵ By specific configurations of external potential²⁶ or strain²⁷, it is possible to access valley polarized current in bilayer graphene. In addition, the valley dependent Hall transport in the presence of electric field was proposed before in Ref.⁷ In this letter we propose a device based on magnetic field and nonuniform strain which could be applied as depicted in Fig. 1.(a),1.(b),1.(c). We study the valley polarization of the sample in the context of Berry curvature. By considering the gap difference between two valley points (K and K') the possible topological valley Hall current and valley polarization are studied.

Methodology

Both strain and magnetic field could be realized as experimental tuning parameters.^{28–31} Although the magnetic field breaks the time reversal symmetry, however, it cannot lift the valley degeneracy. Simultaneous presence of magnetic field and strain in gapped graphene leads to a gap difference between two valleys. Despite the various proposals where have been based on combinations of strain, magnetic and electric fields^{13–16, 18} in the current study, the proposed sample is based on a magnetic field and a nonuniform strain. The valley-resolved Hamiltonian in k -space reads

$$H_{gr}^{\eta}(k) = \hat{\Psi}_{\eta,k}^{\dagger} v_f (\eta \tau_x k_x + \tau_y k_y) \hat{\Psi}_{\eta,k} \quad (1)$$

where v_f is Fermi velocity, the valley index η is $+$ ($-$) for K (K') and the matrices of τ act on sub-lattice indices (A and B). The strain and real magnetic field contributions in k -space given by

$$H_S^{\eta}(k) = \hat{\Psi}_{\eta,k}^{\dagger} v_f (\tau_x A_{S_x} + \eta \tau_y A_{S_y}) \hat{\Psi}_{\eta,k} \quad (2)$$

$$H_M^{\eta}(k) = \sum_q \hat{\Psi}_{\eta,k+q}^{\dagger} v_f (\eta \tau_x A_{M_x} + \tau_y A_{M_y}) \hat{\Psi}_{\eta,k} = \sum_q \mathcal{H}_M^{\eta k}(q),$$

where A_S is the fictitious gauge field due to the strain and A_M is the real magnetic gauge fields (see supplementary information). we have defined

$$\mathcal{H}_M^{\eta k}(q) = \hat{\Psi}_{\eta,k+q}^{\dagger} v_f (\eta \tau_x A_{M_x} + \tau_y A_{M_y}) \hat{\Psi}_{\eta,k}, \quad (3)$$

in which $\mathcal{H}_M^{\eta k}(q)$ stands for the magnetic field induced momentum transfer of q . Finally the k -space mass term is expressed as

$$H_{mass}^{\eta}(k) = \hat{\Psi}_{\eta,k}^{\dagger} (m \tau_z) \hat{\Psi}_{\eta,k}. \quad (4)$$

From theoretical point of view a gap opening in the presence of non-uniform strain is,³² $H_{mass} \propto B^{ps} = (\partial_y(u_{xx} - u_{yy}) + 2\partial_x u_{xy}) \tau_z$. The energy gap as function of pseudomagnetic field is the Zeeman coupling of pseudospin to the associated pseudomagnetic field,³² $E_{Zeeman} = \frac{3}{8} V' a^2 B^{ps}$ where a is the lattice constant, and $V' = 6(eV/\text{\AA})$.³³

It should be noted that the nature of the magnetic and strain dependent gauges are quite different. The magnetic gauge field depends on electronic positions, however, the strain induced gauge is a function of the atomic positions (u_{α}). Unlike the other contributing terms in the Hamiltonian since the magnetic vector potential depends on electrons position in real space, therefore, the Hamiltonian of magnetic field, as indicated in Eq. (3), contains momentum transfer contributions and cannot be represented in block diagonal form of independent k subspaces. However, within the first order perturbation approach, in which the momentum transferring terms cannot contribute, it can be shown that the previous results could be considered reliable at the qualitative level.¹⁸ Unlike the first order correction, momentum transferring terms contribute in the higher orders of the perturbation and generally used block diagonalization approach cannot give rise to an exact answer. Then the non-perturbative part of the strained graphene Hamiltonian is

$$H^{(0)} = \sum_{\eta} (H_{gr}^{\eta} + H_{mass}^{\eta} + H_S^{\eta}). \quad (5)$$

The matrix representation of $H^{(0)}$ in the following k -space basis

$$\hat{\Psi}_k = \begin{pmatrix} \hat{\Psi}_{kA}^+ \\ \hat{\Psi}_{kB}^+ \\ \hat{\Psi}_{kA}^- \\ \hat{\Psi}_{kB}^- \end{pmatrix}, \quad (6)$$

can be written as

$$H^{(0)} = \begin{bmatrix} m & P^- & 0 & 0 \\ P^+ & -m & 0 & 0 \\ 0 & 0 & -m & Q^- \\ 0 & 0 & Q^+ & m \end{bmatrix}. \quad (7)$$

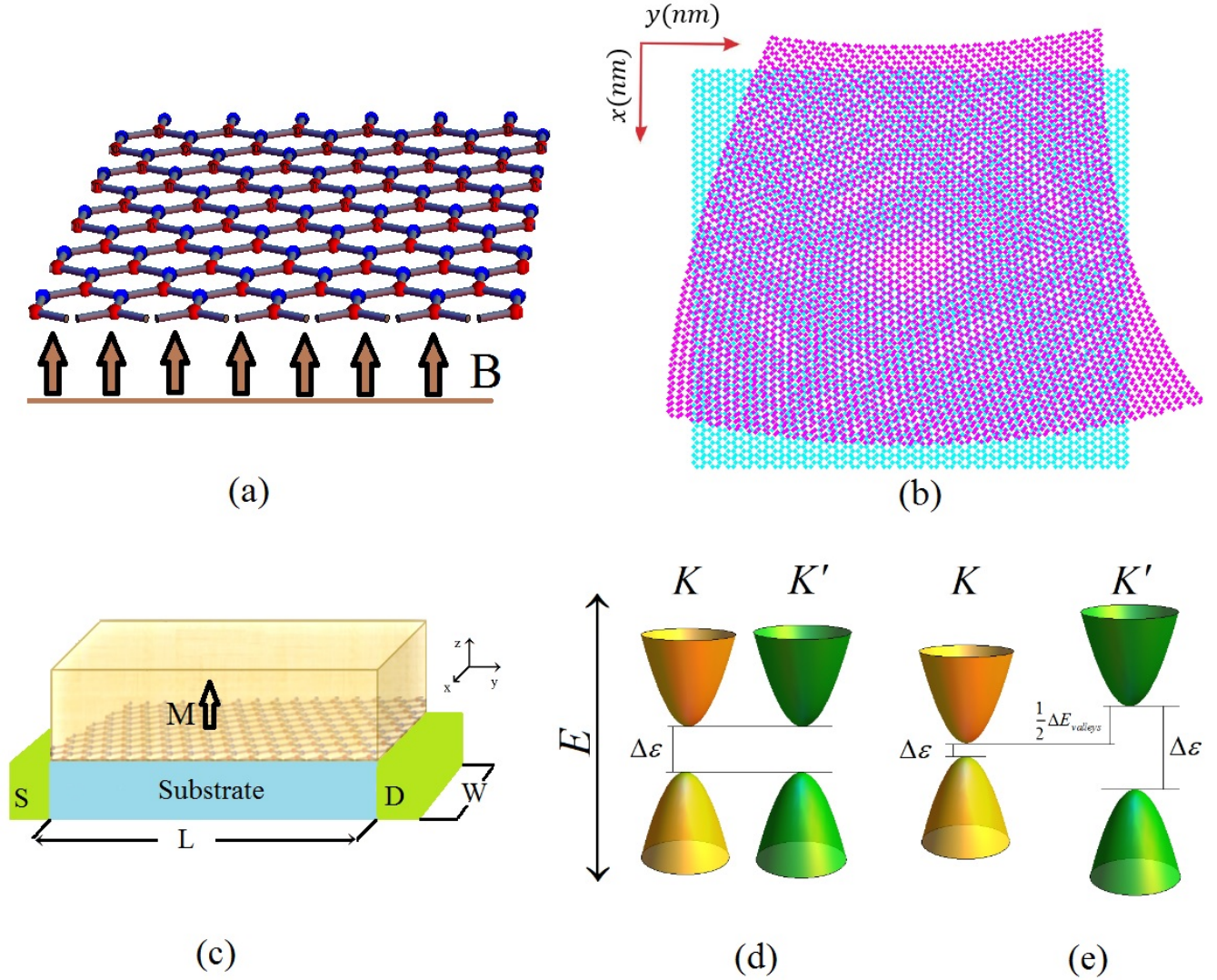


Figure 1. (Color online) (a) Gapped graphene sample in the presence of magnetic field, (b) gapped graphene sample under proposed deformation, (c) a schematic proposal for the valley Hall current and valley polarization in graphene. A ferromagnetic metal with z direction of magnetization has been placed on top. The central region is the strained graphene (the special form of strain is imposed by substrate). The S and D are the source and drain respectively. W and L are the width and length of strained graphene (d), (e) The valley gap difference (VGP) created in a gapped graphene in the presence of electromagnetic field and strain. (d) When the system has a spectral gap ($\Delta\epsilon$) around each of valleys, K and K' . In the absence of magnetic field in the sample, the strain alone could not generate any gap difference between these valley points in $k_f = 0$, where k_f is the radius of the Fermi circle. As illustrated the value of spectral gaps in two valleys are equal. (e) Applying a magnetic field in strained graphene, induces a gap difference $\Delta E_{valleys}$ between the valleys. For typical parameters of $A_{S_x} = 2A_{S_y} = -0.008$ eV, $A_{M_x} = A_{M_y} = 0.0024$ eV, $m = 5$ meV, $\Delta\epsilon_K^0 = 0.0206$ eV, $\Delta\epsilon_{K'}^0 = 0.0616$ eV the gap difference is $\Delta E_{valleys} = 0.041$ eV. For more information about two gauges of strain A_S and magnetic field A_M see the supplementary information.

where $P^\pm = v_f(k^\pm + A_s^\pm)$, $Q^\pm = -v_f(k^\pm - A_s^\pm)$, $k^\pm = k_x \pm ik_y$ and $A_s^\pm = A_{S_x} \pm iA_{S_y}$. First order perturbation accounts for the zero momentum transfer contribution of the magnetic field. Therefore it can be described as

$$H^{(1)} = \sum_{\eta} \mathcal{H}_M^{\eta k}(0). \quad (8)$$

This can be represented in a single k-block of the given basis in the following form

$$H^{(1)} = \begin{bmatrix} 0 & ev_f A_M^- & 0 & 0 \\ ev_f A_M^+ & 0 & 0 & 0 \\ 0 & 0 & 0 & -ev_f A_M^- \\ 0 & 0 & -ev_f A_M^+ & 0 \end{bmatrix} \quad (9)$$

where $A_M^\pm = A_{M_x} \pm iA_{M_y}$. The full Hamiltonian up to the first order perturbation could be written as,

$$H = H^{(0)} + H^{(1)}. \quad (10)$$

It should be noted that as mentioned before $H^{(1)}$ corresponds to the first order corrections and the higher orders of perturbative corrections can be achieved by taking into account the non-zero momentum transfer contributions. The gap difference between two valleys, K and K' , can be obtained within the perturbation theory (see supplementary information). It can be shown that in strained graphene this valley gap difference depends on both magnetic field and applied strain. Within the first order perturbation valley gap difference, which has been defined as $\Delta E_{VGD} = E_K^{gap} - E_{K'}^{gap}$, can be easily found to be

$$\Delta E_{VGD} = \frac{ev_f BL^2}{2} \sum_{\eta} (\mathcal{M}_{+\eta} - \mathcal{M}_{-\eta}) \neq 0 \quad (11)$$

where $\mathcal{M}_{\tau\eta} = \mathcal{C}_{\tau\eta} + \mathcal{C}_{\tau\eta}^*$ and $\mathcal{C}_{\tau\eta} = \alpha_{\tau\eta} \beta_{\tau\eta}^*$. The external magnetic field is denoted by B and L stands for the size of the system. The α and β are the components of the unperturbed Dirac Hamiltonian eigenvectors, $\psi_{\eta}^{(0)}$ and (see supplementary information for more details),

$$\mathcal{E}_{\eta, \mathbf{k}}^{(0)\pm} = \pm \sqrt{m^2 + v_f^2 (k^+ + \eta A_s^+) (k^- + \eta A_s^-)} \quad (12)$$

As illustrated in Figs. 1.d and 1.e the valley gap difference has been appeared as a result of the magnetic field and strain. It is very important to note that Eq. (12) indicates that for a given $\mathbf{k} \neq 0$ state we have $\mathcal{E}_{K, \mathbf{k}}^{(0)\pm} \neq \mathcal{E}_{K', \mathbf{k}}^{(0)\pm}$ even at zero magnetic field. This means that there is a strain induced population imbalance between different valleys at $B = 0$. It has also been realized that the strain moves the Dirac points slightly. Meanwhile, this movement does not change the direct band gap of graphene. A valley Hall current can be generated by the population imbalance as a consequence of the valley gap difference. We have proposed a practical method for measuring the valley Hall current in Fig. 1.c that could be available using the present experimental techniques. By means of this setup, we demonstrated that the valley polarized current can be achieved in strained graphene in the presence of magnetic field which can be expressed in terms of Berry curvature. The topological response to an external gauge field could be obtained by integrating of Berry curvature of filled bands over the momentum space,³⁴

$$\sigma_{xy} = \sum_{\eta} \frac{e^2}{2\pi h} \int \int dk_x dk_y \Omega_{k_x k_y}^{\eta} \quad (13)$$

The Berry curvature $\Omega_{k_x k_y}^{\eta}$ of strained graphene in the presence of magnetic field is (see supplementary information),

$$\Omega_{k_x k_y}^{\eta} = \frac{\eta m v_f^2}{(v_f^2 \pi_x^2 + v_f^2 \pi_y^2 + m^2)^{\frac{3}{2}}} \quad (14)$$

where $\pi_x = k_x + eA_{M_x} + \eta A_{S_x}$, $\pi_y = k_y + eA_{M_y} + \eta A_{S_y}$. Dependence of Berry curvature to gauge fields is shown in figures 2.a, 2.b and 2.c. Fig. 2.a shows the Berry curvature of the system in the absence of any gauge fields.

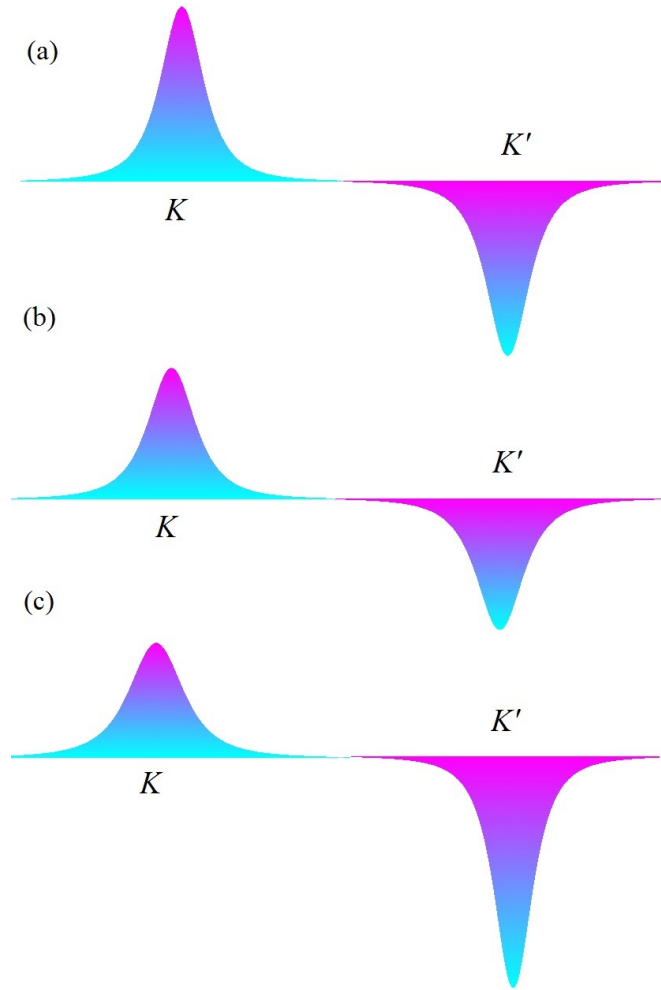


Figure 2. (Color online) Berry curvature of two valley points K and K' . (a) In the absence of strain and magnetic field the Berry curvature of two K and K' are $\Omega^K(k, 0, 0) = -\Omega^{K'}(k, 0, 0)$, (b) in the presence of magnetic field $\Omega^K(k, A_m, 0) = -\Omega^{K'}(k, A_m, 0)$, (c) in the presence of magnetic field and strain $\Omega^K(k, A_m, A_s) \neq -\Omega^{K'}(k, A_m, A_s)$.

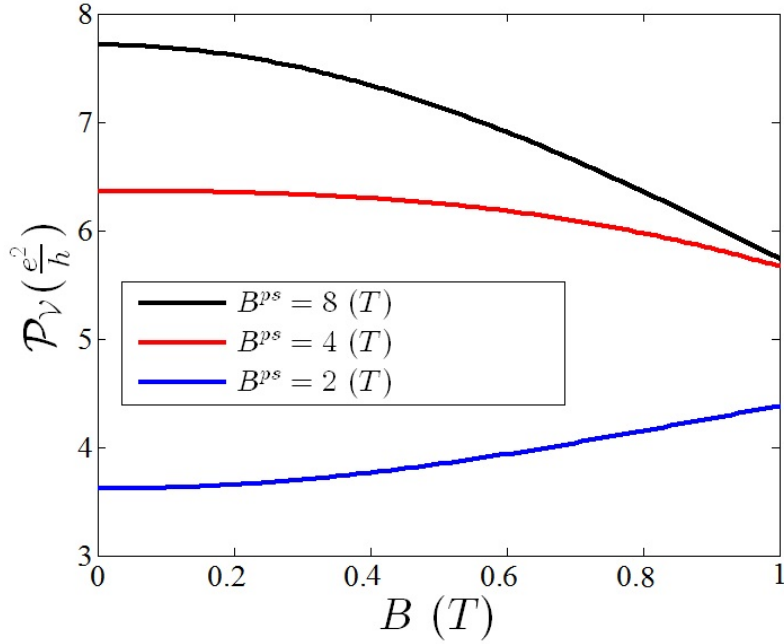


Figure 3. (Color online) Valley polarization function in terms of magnetic field. The nonzero \mathcal{P}_V at zero magnetic field ($B = 0$) arises as a result of the population imbalance induced by nonzero strain when the radius of each of the Fermi circles is not zero. The B^{ps} is the value of pseudo magnetic field which generate by introduced non-uniform strain (the details are presented in supplementary information)

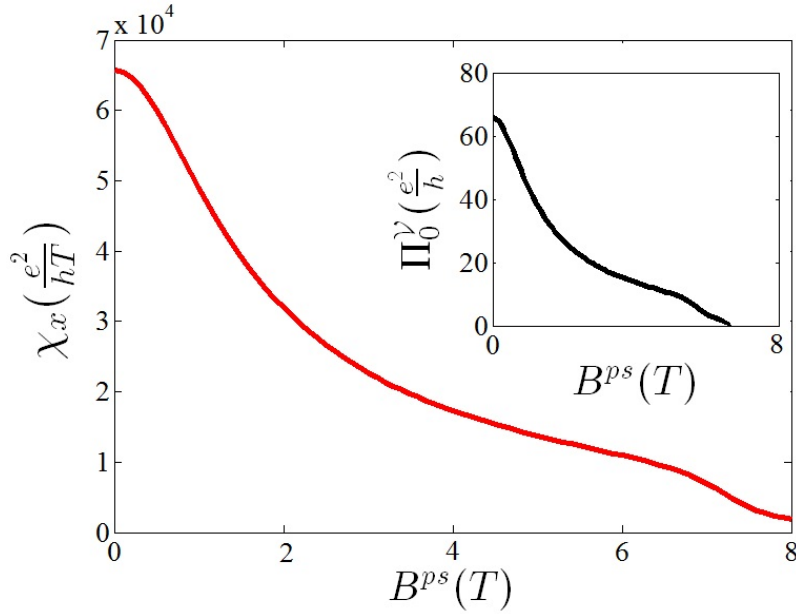


Figure 4. (Color online) Linear response function of valley polarization in terms of pseudo magnetic field. (inset) Magnetic free polarization function (Π_0^V) in terms of pseudo magnetic field.

Results and discussion

In the absence of the strain, there is not any gap difference between two valleys ($E_K^{gap} = E_{K'}^{gap}$). Using the relations which were presented in Eqs. 13 and 14 it can be inferred that the charge conductivity of inequivalent valleys satisfy $\sigma_{xy}^{KC} = -\sigma_{xy}^{K'C}$. Where $\sigma_{xy}^{\eta C}$ is the contribution of the η -valley in the charge Hall conductivity. Meanwhile, the valley resolved current with a given valley index, η , can be defined by $j_{\mathcal{V}}^{\eta} = \langle \eta v \rangle$ where v is the velocity operator. Accordingly, $j_{\mathcal{V}}^{\eta} = \eta j_C$ where j_C is the charge current. The valley polarization in the presence of the external magnetic field is then given by $\mathcal{P}_{\mathcal{V}}^M = \sigma_{\mathcal{V}}^K - \sigma_{\mathcal{V}}^{K'}$ where the valley conductivity $\sigma_{\mathcal{V}}^{\eta} = \eta \sigma_C^{\eta}$.

As long as the population balance between the two valley points is maintained, valley current cannot be induced in the sample. Valley population imbalance can be achieved when the chemical potential of inequivalent Dirac points are not the same where for the strained graphene and in the presence of magnetic field this is really the case. It should be mentioned that valley population imbalance has been employed for generation of valley current in the presence of magnetic field in strained graphene as described in Ref.¹⁸ Furthermore, realization of the valley Hall current strongly depends on population imbalance at different valleys.⁷ Accordingly, the population imbalance that comes from the coexistence of real and pseudo-magnetic fields¹⁸ automatically guaranties the generation of valley polarization in strained valley Hall systems. In the present work it was shown that when the Fermi energy has not exactly been located at Dirac points the strain itself could results in population imbalance and magnetic free valley polarization.

Since the Berry curvatures of different valleys have opposite sign then the Berry curvature dependent quantities such as Hall conductivity vanishes identically once the population balance is established. This is the key point for generation of topological valley current in the system. Using the Eq. 14 it can be shown that, in the absence of the strain, Berry curvature of different Dirac points in the presence of an external magnetic field are opposite. In the other words the total charge conductivity vanishes exactly i.e. $\sigma_{xy}^{KC} + \sigma_{xy}^{K'C} = 0$ ²⁵ (or equivalently valley Hall polarization vanishes $\sigma_{\mathcal{V}}^K - \sigma_{\mathcal{V}}^{K'} = 0$). Unlike the strained sample in this case the position of the Fermi energy cannot result in non-zero charge conductivity. In strained honeycomb structure, the presence of magnetic field induces a gap difference between two valley points ($\Delta E_{VGD} \neq 0$). This gap difference leads population imbalance in two inequivalent Dirac points. Meanwhile unlike the previous case, the Berry curvature of each valleys doesn't contribute oppositely and therefore $\sigma^{CK} \neq -\sigma^{CK'}$,

$$\mathcal{P}_{\mathcal{V}} = \sigma_{\mathcal{V}}^K - \sigma_{\mathcal{V}}^{K'} \neq 0. \quad (15)$$

In the absence of the magnetic field the total conductivity vanishes just when the Fermi energy is exactly located at the Dirac points (which has been indicated by $k_x = 0$ and $k_y = 0$ in Eq. 14 which indicates the contribution of the Dirac points). In Fig. 3 the valley polarization of strained graphene has been depicted in terms of magnetic field. By increasing the value of magnetic fields, functionality of valley polarization for each value of B^{ps} changes in different way. It should be noted that the zero magnetic polarization which has been shown in this figure comes from the strain induced population imbalance in nonzero Fermi circle as discussed before. We have chosen $E_F \simeq 0.1\text{eV}$ that corresponds to n-type doping with conduction electron density about $n \simeq 7.3 \times 10^{11} \text{cm}^{-2}$ and Fermi wave vector $k_f \simeq 0.0152 \text{\AA}^{-1}$.

The linear valley polarization response function, $\chi_{\alpha\beta}$, could be obtained in the presence of magnetic field. In this case the valley polarization can be given by $\mathcal{P}_{\mathcal{V}\alpha} = \chi_{\alpha\beta} \cdot A_{m\beta}$. At the limit of low magnetic fields by expanding each valley resolved Berry curvatures around $A_M = 0$. With the assumption of $A_S > A_M$ we have $\mathcal{P}_{\mathcal{V}} = \Pi_0^{\mathcal{V}} + \chi_{\alpha} \delta A_{M\alpha}$ where $\Pi_0^{\mathcal{V}}$ is the magnetic free polarization and $\chi_{\alpha}^{\mathcal{V}}$ is linear response function of the strained system. After expansion,

$$\Omega_k(A_m, A_s) = \Omega_k(0, A_s) + \frac{\partial \Omega_k(A_m, A_s)}{\partial A_{m_x}} \Big|_{A_{m_x}=0} \delta A_{m_x} + \frac{\partial \Omega_k(A_m, A_s)}{\partial A_{m_y}} \Big|_{A_{m_y}=0} \delta A_{m_y} \quad (16)$$

substituting Eq. 16 in Eq. 13 and integrating, the magnetic free valley polarization and linear response function of the system can be obtained as

$$\begin{aligned} \Pi_0^{\mathcal{V}} &= \frac{e^2}{2\pi h} \sum_{\eta} \int \int dk_x dk_y \Omega_{k_x k_y}^{\eta}(0, A_s) \\ \chi_{\alpha}^{\mathcal{V}} &= \frac{e^2}{2\pi h} \sum_{\eta} \int \int dk_x dk_y \frac{\partial \Omega_{k_x k_y}^{\eta}(A_m, A_s)}{\partial A_{m\alpha}} \Big|_{A_{m\alpha}=0}. \end{aligned} \quad (17)$$

Within a numerical calculation it can be shown that, depending on the value of the Fermi energy, the magnetic free valley polarization $\Pi_0^{\mathcal{V}}$ cannot go all the way to zero. Fig. 4 (inset) shows the magnetic free polarization in terms of pseudo magnetic field. The linear response function of the magnetic field induced polarization, χ_{α} , in terms of the B^{ps} has also been illustrated in

Fig. 4. It should be mentioned that because of the symmetric form of magnetic gauge field within the Dirac cone approximation, in which the band anisotropy of the sample has been ignored, the behavior of χ_y is expected to be identical with χ_x . Strong magnetic field modifies the electronic spectrum and forms Landau levels. In this case, the magnetic field itself induces valley density polarization in the presence of non-vanishing intrinsic orbital magnetic moment.³⁵ Since the Landau levels of two-dimensional structures are localized states, therefore this polarized density could not be extracted from the system. However the external magnetic field here in the present case is weak enough that cannot change the spectrum significantly. In addition we have shown that the population imbalance can be induced by deformation gauge even at zero magnetic field.

Berry curvature dependent quantities can arise provided that the inversion symmetry is broken. Meanwhile since the contribution of each valley has been canceled out by its counterpart there is no valley polarization in the graphene based Hall current system. Meanwhile as discussed in the current study strain could induce population imbalance between different Dirac points when the radius of the Fermi circle is not zero. Since the valley degeneracy has been lifted by the strain for $\mathbf{k} \neq 0$ even at $B = 0$. This is due to the fact that in the presence of the strain we have $\mathcal{E}_{K,\mathbf{k}}^{(0)\pm} \neq \mathcal{E}_{K',\mathbf{k}}^{(0)\pm}$. This means that when the energy of the Fermi level does not exactly meet the Dirac points there is a population imbalance between two nonequivalent Dirac cones. Therefore in this case valley polarized Berry curvature dependent quantities, such as valley polarized Hall conductivity, could be realized as a result of this population imbalance.

References

1. Rycerz, A., Tworzydło, J. & Beenakker, C. Valley filter and valley valve in graphene. *Nature Physics* **3**, 172–175 (2007).
2. Isberg, J. *et al.* Generation, transport and detection of valley-polarized electrons in diamond. *Nature materials* **12**, 760–764 (2013).
3. Zhu, Z., Collaudin, A., Fauqué, B., Kang, W. & Behnia, K. Field-induced polarization of Dirac valleys in bismuth. *Nature Physics* **8**, 89–94 (2012).
4. Goswami, S. *et al.* Controllable valley splitting in silicon quantum devices. *Nature Physics* **3**, 41–45 (2007).
5. Yang, C. *et al.* Spin-valley lifetimes in a silicon quantum dot with tunable valley splitting. *Nature communications* **4** (2013).
6. Salfi, J. *et al.* Spatially resolving valley quantum interference of a donor in silicon. *Nature materials* **13**, 605–610 (2014).
7. Xiao, D., Yao, W. & Niu, Q. Valley-contrasting physics in graphene: magnetic moment and topological transport. *Physical review letters* **99**, 236809 (2007).
8. Sui, M. *et al.* Gate-tunable topological valley transport in bilayer graphene. *Nature Physics* **11**, 1027–1031 (2015).
9. Shimazaki, Y. *et al.* Generation and detection of pure valley current by electrically induced Berry curvature in bilayer graphene. *Nature Physics* **11**, 1032–1036 (2015).
10. Schaibley, J. R. *et al.* Valleytronics in 2d materials. *Nature Reviews Materials* **1**, 16055 (2016).
11. Moldovan, D., Ramezani Masir, M., Covaci, L. & Peeters, F. M. Resonant valley filtering of massive Dirac electrons. *Phys. Rev. B* **86**, 115431 (2012).
12. Grujić, M. M., Tadić, M. Ž. & Peeters, F. M. Spin-valley filtering in strained graphene structures with artificially induced carrier mass and spin-orbit coupling. *Physical review letters* **113**, 046601 (2014).
13. Low, T. & Guinea, F. Strain-induced pseudomagnetic field for novel graphene electronics. *Nano letters* **10**, 3551–3554 (2010).
14. Fujita, T., Jalil, M. & Tan, S. Valley filter in strain engineered graphene. *Applied Physics Letters* **97**, 043508 (2010).
15. Zhai, F., Ma, Y. & Zhang, Y.-T. A valley-filtering switch based on strained graphene. *Journal of Physics: Condensed Matter* **23**, 385302 (2011).
16. Zhai, F., Zhao, X., Chang, K. & Xu, H. Magnetic barrier on strained graphene: A possible valley filter. *Physical Review B* **82**, 115442 (2010).
17. Chaves, A., Covaci, L., Rakhimov, K. Y., Farias, G. A. & Peeters, F. M. Wave-packet dynamics and valley filter in strained graphene. *Phys. Rev. B* **82**, 205430 (2010).
18. Wu, Q.-P., Liu, Z.-F., Chen, A.-X., Xiao, X.-B. & Liu, Z.-M. Full valley and spin polarizations in strained graphene with Rashba spin orbit coupling and magnetic barrier. *Scientific reports* **6** (2016).
19. Jiang, Y., Low, T., Chang, K., Katsnelson, M. I. & Guinea, F. Generation of pure bulk valley current in graphene. *Physical review letters* **110**, 046601 (2013).

20. Wang, J., Chan, K. & Lin, Z. Quantum pumping of valley current in strain engineered graphene. *Applied Physics Letters* **104**, 013105 (2014).
21. Levy, N. *et al.* Strain-induced pseudo-magnetic fields greater than 300 tesla in graphene nanobubbles. *Science* **329**, 544–547 (2010).
22. Klimov, N. N. *et al.* Electromechanical properties of graphene drumheads. *Science* **336**, 1557–1561 (2012).
23. Zhu, S., Stroschio, J. A. & Li, T. Programmable extreme pseudomagnetic fields in graphene by a uniaxial stretch. *Physical review letters* **115**, 245501 (2015).
24. Arias, E., Hernández, A. R. & Lewenkopf, C. Gauge fields in graphene with nonuniform elastic deformations: A quantum field theory approach. *Physical Review B* **92**, 245110 (2015).
25. Vaezi, A., Abedpour, N., Asgari, R., Cortijo, A. & Vozmediano, M. A. Topological electric current from time-dependent elastic deformations in graphene. *Physical Review B* **88**, 125406 (2013).
26. da Costa, D., Chaves, A., Sena, S., Farias, G. & Peeters, F. Valley filtering using electrostatic potentials in bilayer graphene. *Physical Review B* **92**, 045417 (2015).
27. Yan, W. *et al.* Strain and curvature induced evolution of electronic band structures in twisted graphene bilayer. *Nature communications* **4** (2013).
28. Neek-Amal, M., Covaci, L. & Peeters, F. Nanoengineered nonuniform strain in graphene using nanopillars. *Physical Review B* **86**, 041405 (2012).
29. Neek-Amal, M. & Peeters, F. Strain-engineered graphene through a nanostructured substrate. i. deformations. *Physical Review B* **85**, 195445 (2012).
30. Neek-Amal, M. & Peeters, F. Strain-engineered graphene through a nanostructured substrate. ii. pseudomagnetic fields. *Physical Review B* **85**, 195446 (2012).
31. Low, T., Jiang, Y., Katsnelson, M. & Guinea, F. Electron pumping in graphene mechanical resonators. *Nano Letters* **12**, 850–854 (2012).
32. Manes, J. L., de Juan, F., Sturla, M. & Vozmediano, M. A. Generalized effective hamiltonian for graphene under nonuniform strain. *Physical Review B* **88**, 155405 (2013).
33. Ferone, R., Wallbank, J. R., Zolyomi, V., McCann, E. & Fal'ko, V. I. Manifestation of lo-la phonons in raman scattering in graphene. *Solid State Communications* **151**, 1071–1074 (2011).
34. Bernevig, B. A. & Hughes, T. L. *Topological insulators and topological superconductors* (Princeton University Press, 2013).
35. Cai, T. *et al.* Magnetic control of the valley degree of freedom of massive dirac fermions with application to transition metal dichalcogenides. *Physical Review B* **88**, 115140 (2013).

Author contributions statement

All authors contributed equally to this work.

Additional information

Competing financial interests: The authors declare no competing financial interests.